TISSUE ENGINEERING: Part C
Volume 21, Number 9, 2015

DOI: 10.1089/ten.tec.2014.0646

termis
Tissue Engineering
& Regenerative Medicine
International Society

METHODS ARTICLE

Juvenile Swine Surgical Alveolar Cleft Model to Test Novel Autologous Stem Cell Therapies

Montserrat Caballero, PhD,[1,*] Justin C. Morse, MD,[2,*] Alexandra E. Halevi, MD,[3] Omri Emodi, DMD,[4] Michael R. Pharaon, MD,[5] Jeyhan S. Wood, MD,[2] and John A. van Aalst, MD, MA[1]

Reconstruction of craniofacial congenital bone defects has historically relied on autologous bone grafts. Engineered bone using mesenchymal stem cells from the umbilical cord on electrospun nanomicrofiber scaffolds offers an alternative to current treatments. This preclinical study presents the development of a juvenile swine model with a surgically created maxillary cleft defect for future testing of tissue-engineered implants for bone generation. Five-week-old pigs ($n=6$) underwent surgically created maxillary (alveolar) defects to determine critical-sized defect and the quality of treatment outcomes with rib, iliac crest cancellous bone, and tissue-engineered scaffolds. Pigs were sacrificed at 1 month. Computed tomography scans were obtained at days 0 and 30, at the time of euthanasia. Histological evaluation was performed on newly formed bone within the surgical defect. A 1 cm surgically created defect healed with no treatment, the 2 cm defect did not heal. A subsequently created 1.7 cm defect, physiologically similar to a congenitally occurring alveolar cleft in humans, from the central incisor to the canine, similarly did not heal. Rib graft treatment did not incorporate into adjacent normal bone; cancellous bone and the tissue-engineered graft healed the critical-sized defect. This work establishes a juvenile swine alveolar cleft model with critical-sized defect approaching 1.7 cm. Both cancellous bone and tissue engineered graft generated bridging bone formation in the surgically created alveolar cleft defect.

Introduction

Craniofacial bone defects in humans occur in 1/250 live births; the most common of these defects is the alveolar (gumline) cleft, associated with cleft lip and palate, which occurs in ~1/700 live births.[1,2] Autologous bone grafts, often obtained from noncraniofacial sources, are used to reconstruct these defects. Historically, these harvest sites have included tibia, rib, and most recently, the iliac crest.[3] Early surgical repair of the alveolar cleft (defined as under a year of age) was historically the standard of treatment; rib graft was harvested and placed within the cleft defect. As these patients matured, it became evident that early treatment led to growth restriction of the surrounding craniofacial skeleton and was predisposed to resorption.[4] As a consequence these patients demonstrated poorer outcomes, requiring additional, more complex, surgeries at skeletal maturity.[5,6] Because of these concerns, an alternative strategy of delaying the graft until mixed dentition (8–10 years of age) came into favor. Cancellous bone from the iliac crest (a marrow-based treatment, in contradistinction to rib, which is a cortical bone-based treatment) has now become the gold standard for treatment of the alveolar cleft.[7] This delay in treatment allows further growth of the craniofacial skeleton, and minimizes growth restriction[8]; the marrow-based treatment allows more favorable and uniform healing of the graft implant site. Disadvantages of this treatment include the need for a second surgical site, donor site morbidities,[9] unpredictable resorption rates,[10] and the need to delay treatment because of insufficient cancellous bone within the iliac crest in younger patients.[3] One unintended result in this delay is persistence of an uncorrected anomaly beyond the age of self-awareness. As the child becomes aware of his/her facial abnormality after 5 years of age, the anomaly increasingly defines the individual, causing potentially detrimental, lifelong psychosocial impact.[11,12] Bone tissue-engineered strategies offer an exciting alternative to address the gap in the current limitation of autologous bone to treat the growing craniofacial skeleton,[13] and will allow treatments without a secondary surgical site, at an

[1]Plastic Surgery, Cincinnati Children's Hospital Medical Center, Cincinnati, Ohio.
[2]Plastic and Reconstructive Surgery, The University of North Carolina School of Medicine, Chapel Hill, North Carolina.
[3]General Surgery, Loyola University Medical Center, Maywood, Illinois.
[4]Oral and Maxillofacial Surgery, Rambam Medical Center, Haifa, Israel.
[5]Plastic Surgery, Kapiolani Hospital for Women and Children, Honolulu, Hawaii.
*These authors contributed equivalently as first authors.

optimal time for the child, no longer limited by the child's age or size. To justify the use of novel tissue-engineered alternatives as a replacement for current human protocols, they must be favorably compared to the current gold standard treatment of the alveolar cleft—cancellous bone grafting—in safety and efficacy.

The development of relevant animal models is required to extrapolate *in vitro* data to *in vivo* results for establishing early, successful novel treatments of pediatric alveolar clefts. Currently, murine animal models are the most common for studying craniofacial bone defects, including the alveolar cleft; however, there are several significant shortcomings in rodent models, such as significant size discrepancy when compared to humans, functional differences of the craniofacial skeleton, and major dissimilarities in wound healing rates. These deficiencies have led to slower than predicted translation to human conditions.[14,15] Though there are several large animal models for the alveolar cleft (goat, sheep, dog, cat, pig, and monkey), many have significant drawbacks, including functional dissimilarities when compared to the human craniofacial skeleton (sheep and dog models), and expense (primate models).[16–19] The swine maxillofacial skeleton though, has multiple functional similarities to humans, largely because swine, like humans, are omnivores; similarities include maxillary, mandibular, and temporomandibular joint function; teeth and surrounding structures; and comparable critical-sized defects and healing rates.[20] Although uncommon, alveolar clefts associated with cleft lip and palate, also congenitally occur in pigs, and resemble alveolar clefts in humans (Fig. 1). An added benefit to using the swine model is the ability to test age-based treatment strategies. There is an $\sim$1 month (swine) to 1 year (human) equivalence that is derived from the timing of central/lateral incisors and canine eruption[21] and development of sexual maturity, which occurs between 9 and 12 months in swine and 10–12 years in humans.[22] This correlation allows for timed interventions in a swine model that correspond to well-characterized ages for treatment in humans.[23] Finally, recent completion of the pig genome project[24] is facilitating the development of human disease models in swine that are currently only found in mice[25]; consequently, development of swine surgical models will be a key step in initiating translational studies that address human conditions. To our knowledge, swine alveolar cleft models are reported in only three publications,[18,19,26] with a single report of a maxillary model to assess bone resorption after onlay bone grafting.[27] None of these models addresses a preclinical scenario to test tissue-engineered stem cell therapies.

In this study, we have developed a swine alveolar cleft model that can be used for testing of tissue-engineered constructs for repair of the alveolar cleft and by extension, other craniofacial bone defects. This model will also serve the purpose of conducting more extensive preclinical studies.

Materials and Methods

Animals

This study was approved by the Institutional Animal Care and Use Committee (IACUC) at the University of North

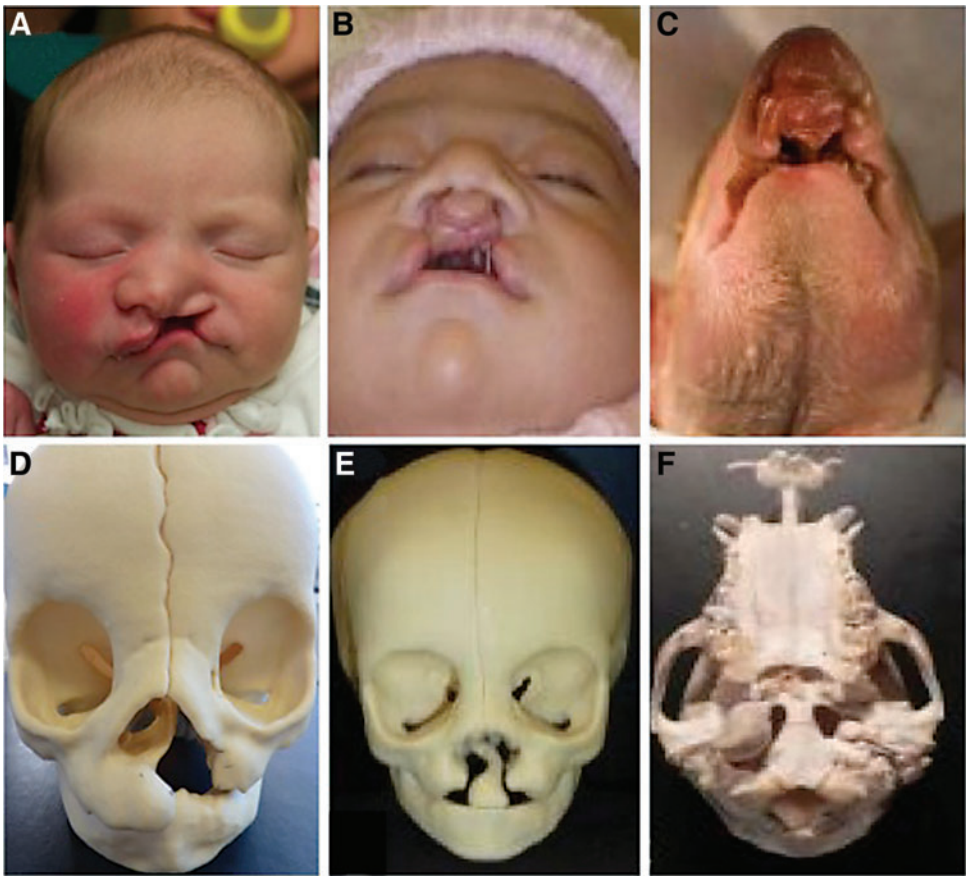

FIG. 1. A child with a left unilateral complete cleft lip and palate **(A)** and bilateral cleft lip and palate **(B)** with skull models of the unilateral **(D)** and bilateral **(E)** defects demonstrating the absence of bone in the maxilla at the alveolar ridge. A piglet cadaver demonstrates a bilateral cleft lip and palate **(C)**, with the skull of the same animal demonstrating absence of bone on either side of the anterior maxillary segment **(F)**. Color images available online at www.liebertpub.com/tec

Carolina (UNC) and North Carolina State University School of Veterinary Medicine (NCSU). All animal care adhered to NIH guidelines. A total of 12 pigs were used to establish a surgical alveolar cleft model. Six cadaveric pigs, which were freshly euthanized following completion of unrelated studies at UNC, were utilized for surgical technique development, including rib and iliac crest cancellous bone harvest (Fig. 2), creation of the alveolar defect (both unilateral and bilateral defects), and placement of the bone grafts within the defect. The survival surgery group included six domestic pigs obtained from the NCSU Swine Educational Unit. The piglets were offspring of (Yorkshire × Landrace × Large White) sows bred to (Hampshire × Duroc × Pietran) boars and were expected to exhibit 100% heterosis. All experimental animals were negative for swine reproductive and respiratory syndrome, mycoplasma hyopneumonia, parvovirus, leptospirosis, hemophilus parasuis, streptococcus suis, swine influenza, and transmissible gastroenteritis. Piglets were marked at birth with an ear notch and tracked for surgery at 5 weeks. Piglets were kept in a 10 × 20 foot room with two pigs per room in a 12/12 light/dark cycle and fed hard pellets (Labdiet Porcine Lab Grower, PMI Nutrition Int'l., LLC). Water was added to soften the pellets for the first 24 h after surgery. Diet enrichment included plastic balls and twice per day combination of the following: apples, bananas, carrots, potatoes, sugar cane, peanut butter, and dried fruit with vegetables. During the first week postsurgery the piglets were fed with medicated 22% protein starter feed instead of the regular feed.

Surgical protocol

Survival surgery was performed on 5- to 6-week-old pigs weighing 10 to 17 Kg. Three swine were left untreated to test critical-sized defects (1.0, 1.71, and 2.0 cm) and three were used for autologous bone graft testing (rib, iliac crest cancellous bone, and tissue-engineered grafts). Animals were anesthetized by intramuscular injection of midazolam (0.5–1 mg/kg) and ketamine (10–20 mg/kg); anesthesia was maintained through the procedure with Isoflurane 0–5% Mask/ET tube. Pigs were placed in a lateral decubitus position, and the face and oral cavity were prepped with betadine, and draped sterilely. Marcaine 0.25% with 1:200,000 epinephrine was injected on the ipsilateral side before defect creation, to decrease intraoperative pain and bleeding. An incision was made to the upper buccal sulcus at the junction of the gingiva and palate mucosa, allowing release of the gingiva (with buccal mucosa) superiorly, exposing the maxilla from the central incisor to the canine. Palate mucosa was also elevated exposing the underlying hard palate to the midline. Once the soft tissue was cleared from the bony landmarks, a 1 cm area (anterior to posterior) was marked on the exposed bone (Fig. 3A), with extension superior to the piriform aperture, and medially to a paramedian position on the hard palate. A reciprocating saw was used to create the osteotomies, first for a 1 cm and then for a 2 cm wide cleft (Fig. 3B). Bone margin was retained over the roots of the central incisor and the canine. All bone was cleared to the nasal mucosa within the piriform aperture, and to a paramedian position on the hard palate. The defect was then either left empty or filled with autologous bone or tissue-engineered grafts (Fig. 3C–E) and the soft tissue of the oral cavity was closed with interrupted vicryl sutures (Fig. 3F). A computed tomography (CT) scan was performed immediately after surgery. Appropriate postoperative antibiotics (ceftiofur 5 mg/kg, cefazolin 22 mg/kg, or ampicillin 20 mg/kg) and analgesia (meloxicam 0.4 mg/kg) were administered for 5 days postsurgery. Piglets resumed normal activities and behavior shortly after awakening from the surgical procedure. For the first 24 h after surgery, feed pellets were softened by adding water. After this, animals were maintained on a regular hard pellet diet with enrichments as described in the Animal Methods section. Piglets were monitored for signs of inflammation and infection during the postoperative period and sacrificed 30 days postsurgery by intravenous injection of 390 mg/mL pentobarbital sodium, dosed at 1 mL/10 lbs. CT scans were performed following euthanasia and ITK-SNAP 3D CT software[28] was used to determine volumetric bone fill, bone bridging, and graft resorption by comparing these CT scans with the ones performed immediately after surgery.

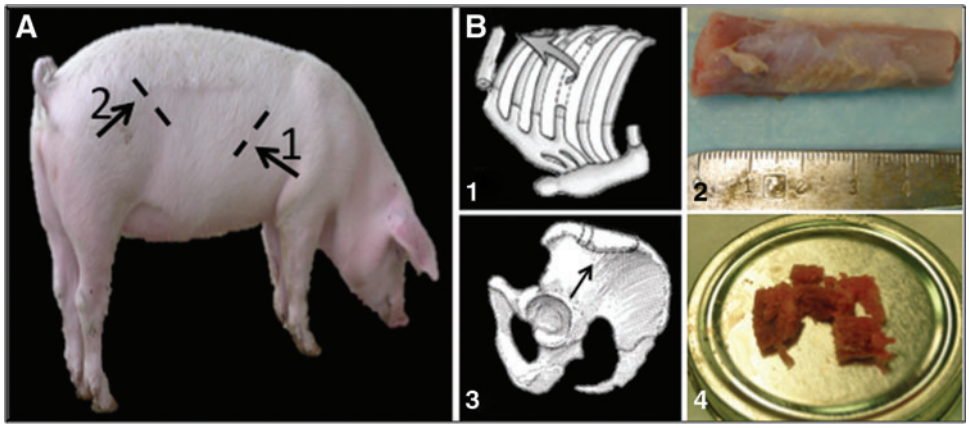

FIG. 2. Cadaver studies were performed on six freshly euthanized animals. **(A)** The surgical markings in A1 demonstrate the site of the skin incision for rib graft harvest (1 cm) and in A2 for iliac crest cancellous bone harvest (2 cm). **(B)** A 5 cm section of rib six was harvested (B1, 2) and the iliac crest was exposed for harvest of cancellous bone (the marrow within the iliac crest, B3, 4) and prepared for implantation. Arrow in **B3** points to the area of the iliac crest accessed for removal of cancellous bone. Color images available online at www.liebertpub.com/tec

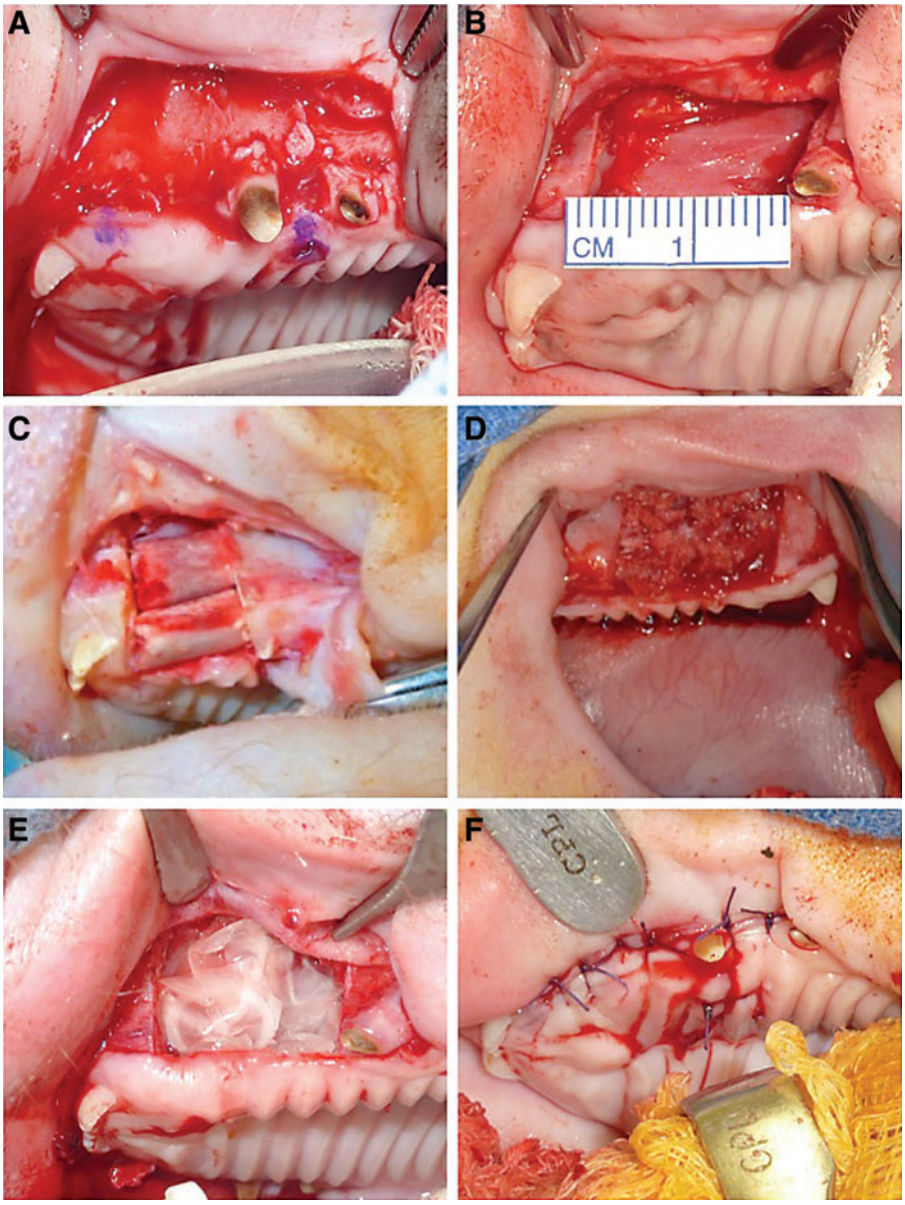

FIG. 3. Surgery on living animals ($n=6$) involved exposure of the unilateral maxilla using an incision at the junction of the gingival mucosa and palate and marking of the osteotomy sites **(A)**, followed by creation of a full-thickness bone defect from the central incisor to the canine, medially extending to the nasal mucosa of the piriform aperture, and to the midline vomer of the palate **(B)**. The rib graft was split to fill the surgically created 1 cm defect **(C)**; cancellous bone was placed into a 2 cm defect **(D)**; tissue-engineered scaffolds were stacked within the defect **(E)**. After placing each test condition within the defect, the wound was closed with absorbable suture **(F)**. Color images available online at www.liebertpub.com/tec

Autologous bone treatments

Rib graft was harvested from rib number 6, using a 1 cm incision, leaving the periosteum intact (Fig. 2A, B1–2). The rib graft was split longitudinally and placed with the cortical component facing outward (Fig. 3C). Iliac crest graft was harvested using a 2 cm incision directly over the anterior superior iliac crest; the cartilage cap of the iliac crest split and lifted with an osteotome exposing the underlying cancellous bone (Fig. 2A, B3–4); bone marrow was harvested using a curette. Sufficient cancellous bone was harvested to fill the alveolar defect (Fig. 3D).

Poly-lactic co-glycolic acid scaffolds preparation

Nanomicrofiber scaffolds (NMFS) were created by electrospinning resorbable Delta System™ poly-lactic co-glycolic acid (PLGA) implants from Stryker®, as previously described.[29] Briefly, PLGA implants were solubilized in 3:1 v/v dichloromethane:dimethyl formamide at 8% wt/v concentration and electrospun at 4.4 kV/inch, with a CO_2 flow rate of 1 L/min, and polymer flow rate of 0.1 mL/h. to create 1 cm diameter scaffolds. Before cell seeding, scaffolds were sterilized in 70% alcohol under UV light for 4 h and primed with growth media for 24 h.

Mesenchymal stem cells isolation

Swine umbilical cords (UC) were harvested at the time of birth and labeled for future identification. UC were immersed in sterile phosphate-buffered saline (PBS) with 300 U/mL penicillin, 300 µg/mL streptomycin, and 0.75 µg/mL amphotericin B and transported in ice to the laboratory. Umbilical cords were cut into pieces and the mesenchymal stem cells (UC MSCs) were isolated from Wharton's Jelly using an explant technique. MSC phenotype was confirmed by the presence of surface markers CD105 (89%), CD90 (99%), CD73 (71%), and the absence of CD34 (<1%),

assayed by flow cytometry, as previously described.[30] Passage 0 cells were seeded at a density of 5×10^3 cells/cm^2, grown in Dulbecco's modified Eagle's medium (DMEM) 15% fetal bovine serum (FBS) and sub-passaged at 80% confluence.

Cell labeling and differentiation

To identify autologous transplanted UC MSCs, cultures were labeled with recombinant Adeno-Associated Virus (rAAV2) System, expressing the enhanced green fluorescence protein (eGFP) under the CMV promoter (obtained from UNC-Vector core). Passage 1 cells were seeded onto PLGA scaffolds at a density of 4×10^4 cells/cm diameter of scaffold. Once MSCs reached 80% confluence, they were incubated for 45 min in DMEM containing glutamine and 0.5×10^{10} particles/mL of rAAV2-eGFP. After the incubation period, media was replaced with osteogenic media ([α]-MEM basal medium supplemented with 10% FBS, 2 mM glutamine, 100 U/mL/100 μg/mL penicillin/streptomycin, 10 mM β-glycerophosphate, 0.1 μm dexamethasone, and 50 μM ascorbic acid)[31,32]; cells were monitored for the presence of fluorescence using a Nikon Eclipse Ti-S inverted microscope. Cells were then seeded onto the PLGA scaffolds and predifferentiated (osteoinduced) for 5 days, then implanted into the swine alveolar cleft model (Fig. 3E).

Histological analysis

Fixed bone samples were decalcified in 10% HCL/EDTA pH 7.4 for 12 h, washed with deionized water, transferred to 70% ethanol, paraffin embedded, and sectioned into 5 μm slides. Deparaffined sections were stained with hematoxylin and eosin to analyze matrix architecture, inflammatory response, bone ingrowth, and cellular organization. Immunohistochemical analysis was performed in contiguous slides using anti-eGFP antibody (Pierce OSS00005W). Antigen retrieval was performed with NaCitrate buffer at 98°C for 40 min and endogenous peroxidase was blocked by incubation with BLOXALL™ for 30 min at room temperature; samples were then incubated with primary antibody overnight at 4°C, washed with PBS-0.1% tween 20, incubated with goat anti-rabbit peroxidase-conjugated antibodies, and developed with Immpact NovaRED peroxidase substrate. Hematoxylin was used for counterstaining. Samples were analyzed using a Nikon Eclipse Ti-S inverted microscope.

Results

Cadaveric work

Six freshly euthanized cadaveric swine were used to establish surgical technique. A 1 cm incision was required to harvest a 5 cm section of rib number 6; a 2 cm incision was required to harvest iliac bone using standard technique to lift the cartilaginous cap, and harvesting the cancellous bone using a curette (Fig. 2A, B). Alveolar clefts were created using a reciprocating saw. Both the unilateral 1 cm and 2 cm defect were created with no evidence of bone instability. Similarly, creation of bilateral 1 cm defects did not create instability of the anterior maxilla; however, a bilateral 2 cm defect resulted in central anterior maxillary segment instability, suggesting that a similar defect in surviving swine would result in postoperative feeding problems.

Placement of rib graft, cancellous bone, and PLGA scaffolds were performed in the 2 cm defects created in the cadaver pigs. A 3 cm rib segment split in two and cancellous bone from the iliac crest was sufficient to fill both the 1 cm and a 2 cm defects (Fig. 3C, D). PLGA scaffolds placed in the 2 cm surgically created defect required a stack of twenty 1 cm diameter scaffolds (Fig. 3E).

Surgical procedure

Six living animals were used to establish the swine alveolar cleft model. The procedure was performed within a 1.5-h time frame; all animals survived surgery. Piglets recovered normal activity within a day after surgery. For the first 24 h after surgery, feed pellets were softened by adding water; with this adjustment in diet, piglets were able to feed and drink without problems shortly after surgery. During the month-long study no infections or other healing problems were reported for any of the subjects and all pigs gained weight at normal rates.

Critical size defect determination

To determine the size of a critical-sized bone defect in 5-week-old piglets, 1 cm (Fig. 4A), 1.7 cm (Fig. 4B), and 2 cm defects (Fig. 4C) were created and left untreated for 1 month (actual order of surgery: 1.0 cm [based on reported critical-sized defect], 2.0 cm, followed by 1.7 cm). CT scans performed at day 30 and analyzed with ITK-SNAP 3D CT

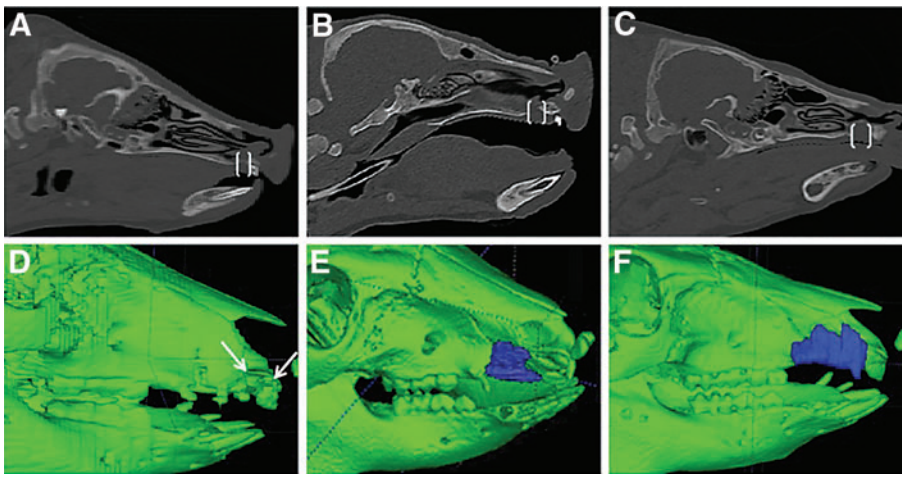

FIG. 4. One centimeter **(A)**, 1.7 cm **(B)** and 2 cm **(C)** surgically created alveolar cleft defects were left untreated in separate swine subjects, then assessed by computed tomography (CT) scan at days 0 and 30. **(A–C)** The day 0 defects are demonstrated with *white brackets*. At day 30, 3D CT scan reconstructions demonstrate bridging bone in the 1 cm defect **(D)** with no or minimal evidence of bone healing in the 1.7 and 2 cm defects **(E, F**; the *blue color* designates absent bone**)**. Arrow designates the extent of the original defect. Color images available online at www.liebertpub.com/tec

Table 1. Weight-Based Critical-Sized Defects Were Determined for All Study Animals

Graft	*Defect size (cm)*	*Weight day 0 (kg)*	*Weight day 30 (kg)*	*Defect size/Weight*[a] *(cm/kg)*
1 cm untreated	1.0	17	31	0.06
2 cm untreated	2.0	10.8	17.5	0.19
1.7 cm untreated	1.7	10	23	0.17
Rib graft	1.0	14	28.5	0.07
Cancellous graft	2.0	11.9	17	0.17
UC MSC-PLGA	1.5	9	18	0.17

Because weight significantly varied for 5-week-old piglets, a normalized defect size was established. Normalization was weight based, and created based on the knowledge that the 2 cm defect in a pig weighing 10.8 kg did not heal. (a) normalized ratio of 0.17 cm/kg.
PLGA, poly-lactic co-glycolic acid; MSC, mesenchymal stem cell; UC, umbilical cords.

software demonstrated complete healing of the 1 cm defect with bone bridging (Fig. 4D), while the 1.7 and 2 cm defect showed a nonhealed bone gap (Fig. 4E, F). Piglet weight, defect size, and normalized defect size by weight for all the experimental subjects are listed in Table 1.

Bone formation and volume fill

One month after surgery the CT scans obtained from a normal maxilla (Fig. 5A, D) were compared to defects treated with rib (Fig. 5B, E) and cancellous bone (Fig. 5C, F); the rib graft did not demonstrate integration with surrounding, intact maxilla (Fig. 5E); the cancellous graft integrated with the surrounding tissue with bridging bone formation detected in the alveolar defect (Fig. 5F). New bone formation and integration with surrounding maxillary bone was also detected at day 30 postsurgery in the defect treated with autologous UC MSC-PLGA implants, as shown in the 3D reconstruction of the CT scan in Figure 6D.

Bone volume calculations were performed using ITK-SNAP software for the cancellous bone (Fig. 6A, C) and UC MSC-PLGA (Fig. 6B, D)-treated defects. The defect treated with UC MSC-PLGA scaffolds showed a slightly better volume fill of the defect, with 37 mm^3/kg (589 mm^3 total) compared with 22 mm^3/kg (389 mm^3 total) for the cancellous bone graft (Fig. 6E).

Histology

Bone formation was evaluated with H&E staining of tissue sections from the treated defects. None of the histological sections demonstrated signs of inflammatory reaction. The rib graft appeared as resorbing compact bone with a rim of osteoclasts surrounding the implanted bone (Fig. 7B); the cancellous bone and the UC MSC-PLGA grafts showed evidence of immature bone formation (Fig. 7C, D), with structural similarity to normal maxillary bone (Fig. 7A) with osteoid, connective tissue, and trabeculations. Immunostaining with anti-GFP antibody revealed the presence of differentiated labeled cells implanted within the UC MSC-PLGA scaffolds associated with the newly generated bone (Fig. 7 E, F).

Discussion

Current surgical techniques for early repair of the alveolar cleft have severe limitations including growth restriction, implant reabsorption, and the need for staged, multiple surgical procedures.[4–7] Delayed repair of the alveolar cleft using cancellous bone from the iliac crest has eliminated growth restriction, but it still requires a secondary surgical site.[7] Tissue-engineered strategies offer a promising alternative to the current treatment strategy, but require proof of equivalence to the current gold standard treatment (or evidence of improved efficacy), and safety, both *in vitro*, and in large animal models, before translation to humans.

Swine models are currently being used in multiple medical and surgical disciplines,[33–36] suggesting that swine models as a proxy for human conditions are reasonable. Further benefits to the use of swine, include recent completion of the swine genome project, with steady increases in the number of swine transgenic models,[37,38] including a green fluorescent protein model[39] and a severe combined immunodeficiency model[40]; these models yield exciting possibilities for preclinical trials in swine that were previously limited to rodent and primate models.[37,41–43]

Anatomic similarities between swine and humans in body size, maxillary bone anatomy, TMJ function[23]; bone remodeling, regeneration, and cortical bone mineralization, and critical-sized bone defects,[44] also suggest that swine craniofacial models that mimic human conditions are also appropriate. Several swine models exist for use in craniofacial conditions including mandibular reconstruction,[33] post traumatic conditions,[36] cranial defects,[35] and nasal and

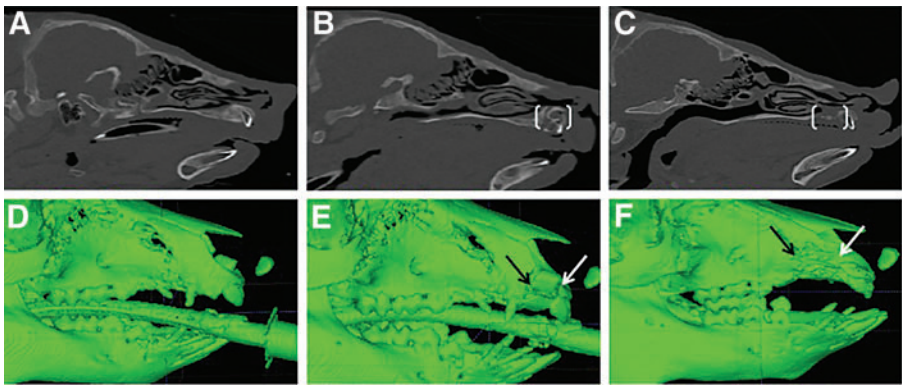

FIG. 5. Day 30 CT scans demonstrate normal swine maxilla **(A, D)** compared to a 1 cm surgically created defect treated with rib graft **(B, E)** and a 2 cm defect treated with cancellous bone **(C, F)**. Rib graft **(E)** exhibited lack of integration to the surrounding normal bone (denoted by the *arrows*), while cancellous bone graft **(F)** demonstrated bridging bone (*arrows*) with integration into the surrounding normal bone. Brackets clarify the location of the bone defect. Color images available online at www.liebertpub.com/tec

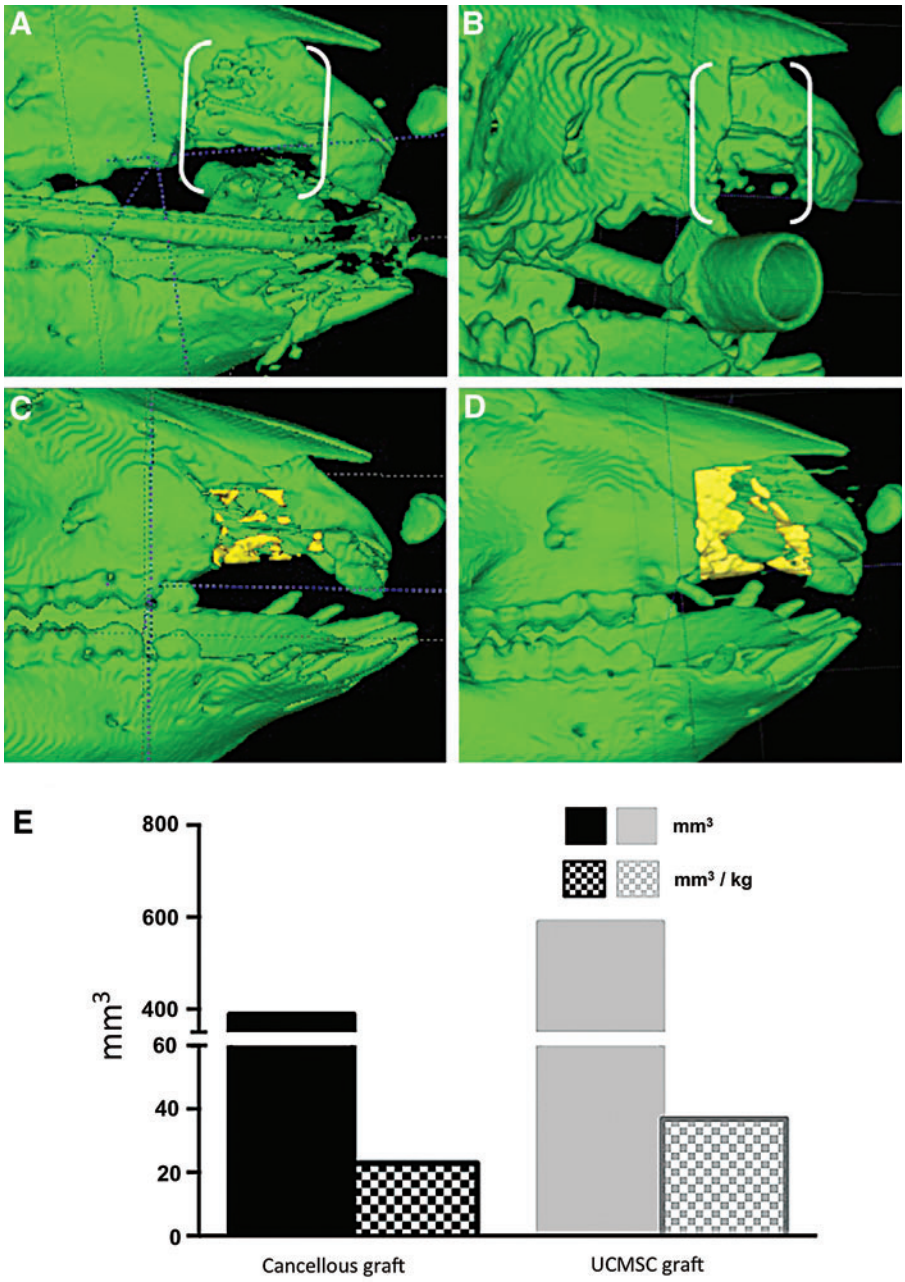

FIG. 6. CT scans demonstrate the surgically created defects at days 0 **(A, B)** and 30 **(C, D)** with new bone generation highlighted in *yellow* after treatment with cancellous bone **(C)** and differentiated UC MSCs on PLGA scaffolds **(D)**. This reconstruction represents a single vertical cut through the bone, and hence only provides a 2D surface area of new bone formation. The total volume of newly generated bone was determined using ITK Snap software **(E)**. UC MSC graft treatment resulted in a larger volume of new bone formation than cancellous bone treatment, in both absolute volume (*solid bars*) and volume normalized by weight (*hashed bars*). PLGA, poly-lactic co-glycolic acid; MSC, mesenchymal stem cell; UC, umbilical cords. Brackets clarify the location of the bone defect. Color images available online at www.liebertpub.com/tec

oral reconstruction[34]; however, only a single study has used a swine model to study a critical-sized maxillary defect, which was treated with distraction osteogenesis.[45] Our study describes the creation of a critical-sized maxillary defect in swine to test novel tissue-engineered therapies.

The human alveolar cleft uniformly occurs in continuity with a cleft of the lip. To mimic this condition exactly in the swine model would have necessitated creating both a cleft lip and alveolus simultaneously. However, concurrent defects in the soft tissue and bone would have resulted in a healing conundrum: closing the newly created soft tissue defect would result in scar tissue, which would have an immediate impact on the healing of alveolar cleft treatments. Leaving the soft tissue defect unrepaired would similarly impact the healing of a treated bone defect. To limit variables affecting treatment of the bone defect, the decision was made to create the bone defect in isolation. Secondarily, a decision was made to use a unilateral alveolar defect rather than a bilateral defect. The pig is an obligate nasal breather; bilateral defects could theoretically result in inflammatory changes in both nostrils, resulting in obstruction leading to an inability to breathe postoperatively. In addition, the instability of the central maxillary segment with bilateral defects approaching 2 cm in size would have caused postoperative feeding problems and impeded bone healing, which requires stability of the surrounding bone structures. The bilateral 1 cm defect—which did not result in maxillary instability—healed without treatment in the first test animal, and hence was not pursued.

The 1 cm surgically created alveolar cleft defect was chosen because this is the reported dimension of a critical-sized defect in swine[22]; however, this defect healed during

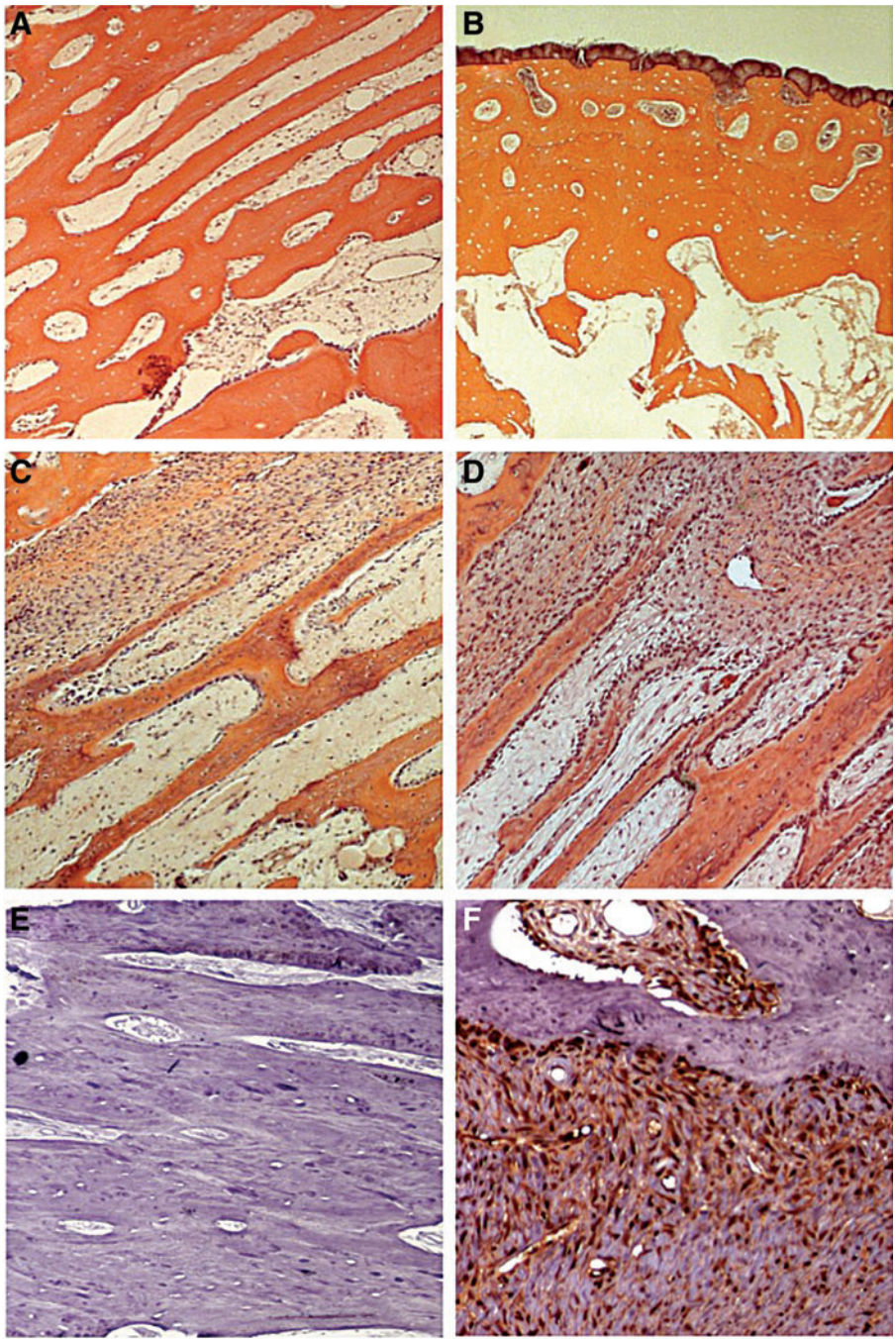

FIG. 7. H&E stains comparing contralateral normal maxilla **(A)** with rib **(B)**, cancellous bone **(C)**, and UC MSC-PLGA grafts **(D)** demonstrate absorbing cortical bone with a rim of osteoclasts, and nonintegration in the rib graft **(B)**. The cancellous graft **(C)** and UCMSC-PLGA **(D)** demonstrate normal appearing bone formation. To determine the presence of UC MSCs in the newly formed bone, normal maxilla **(E)** was compared to the newly formed bone with UC MSCs labeled with AAv-GFP **(F)**. GFP-positive cells (stained in *red*) are present in the areas of new bone formation within the treated defect, indicating the presence of implanted UC MSCs; no background staining is noted in normal bone. Pictures shown for treatments correspond to the center of the defect. No host bone is shown. Color images available online at www.liebertpub.com/tec

the 1-month evaluation period. This finding was not altogether surprising because juveniles have greater healing capacity than adults, both in swine and in humans.[46,47] The 2 cm defect was chosen as a larger sized defect that would not compromise maxillary stability (as determined by our cadaver work). Though this defect did not heal, the size of this defect was problematic in smaller piglets. Because of variation in the size of 5-week-old piglets (with weight variations from 9.0–17 kg), a 2 cm defect would involve a significant portion of the hemi maxilla, and it would be well beyond the borders of a congenitally occurring alveolar cleft defect in both humans and pigs (which should extend from the central incisor to the canine; Fig. 1). Given these considerations, our next surgically created defect was made as large as possible, but maintained between the central incisor and canine. This defect size was 1.71 cm in a 10 kg pig. To create standardized defects in pigs, normalizing for weight is a logical choice because pig weight gain correlates directly to maxillary size,[22] a finding that was confirmed in our cohort of piglets (data not shown). Given that the 1.71 cm defect in a 10 kg pig was critical sized the remainder of the study animals underwent creation of defects that were 0.17 cm/kg (Table 1).

To compare treatment outcomes, we utilized rib graft (historical treatment), cancellous bone graft (current gold standard treatment), and UC MSC-PLGA NMFS (a novel tissue-engineered construct). In our juvenile swine model, the rib graft did not integrate with the surrounding tissue; histological

analysis revealed compact mature bone (still present from the original implanted rib) with osteoclasts lining the surface of the graft, a signal of bone reabsorption. This finding corroborates historical problems associated with this treatment in humans, including lack of integration and bone reabsorption.[3]

Cancellous bone grafting is the current gold standard treatment for the human alveolar cleft. This is a marrow-based treatment that results in improved bone generation and retention in the cleft.[48] Treatment of the surgically created alveolar cleft defect with cancellous bone graft demonstrated integration with the surrounding bone and appropriate volume filling of the defect. Histological examination demonstrated woven, immature bone resembling the surrounding intact maxillary bone and correlates with findings in humans.[48,49]

The alveolar cleft is a relatively limited bone defect, but it is representative of many other larger craniofacial bone defects. If an engineered bone protocol can be determined as safe and efficacious for the alveolar cleft, it will have far-reaching consequences for treatment of a variety of craniofacial defects. The immediate benefit of our approach using autologous UC MSCs on PLGA electrospun NMFS is that UC harvest is both noninvasive and noncontroversial, yielding a high number of plastic MSCs.[50] The value of these MSCs is currently being tested worldwide in 55 open clinical trials using transplantation or infusion protocols for diseases including diabetes mellitus, Alzheimer's disease, acute burn, liver cirrhosis, and cardiomyopathy.[51] Furthermore, a limited but growing literature examining porcine MSCs has demonstrated function similar to human MSCs.[52]

The scaffolds used in our studies were electrospun from Stryker Delta resorbable plates (PLGA), which are FDA approved for use in pediatric patients. These plates are both nonimmunogenic and biodegradable. We have previously demonstrated that these electrospun scaffolds support MSC attachment, migration, proliferation, osteogenic differentiation, and matrix deposition[30,53]; work by others has demonstrated adequate structural support for treating bone defects *in vivo*.[54,55] In this study, bone generated using differentiated UC MSCs on PLGA NMFS was better (though not statistically significant) by CT volumetric analysis and histologically similar to the bone generated using cancellous bone from the iliac crest. In the tissue-engineered treatment, histology demonstrated no evidence of reabsorption or inflammation within the graft site. The preliminary indication, based on the anti-GFP antibody findings, is that the differentiated UC MSCs are present and contribute to bone formation within the surgically created cleft. Taken together, these findings suggest that autologous UC MSC-based tissue-engineered scaffolds are a promising treatment option for the alveolar cleft.

There are some limitations to our findings. A more critical examination of the CT scan demonstrates incomplete fill of the cleft with newly generated bone. Because complete bridging bone across the cleft is the desired outcome of our study, we need to develop strategies to improve bone fill of the defect. The change to our protocol most likely to generate this improvement is an increased time course of healing. We are currently performing studies that will allow follow-up of 3 and 6 months to allow maturation of newly developed bone. Increased duration of the study will also improve the accuracy of 3D CT software analysis. ITK-SNAP 3D reconstruction software is based on attenuation labeling, which is directly related to calcium content of the bone; the ability to differentiate bone from surrounding soft tissue increases as bone matures. Lastly, the sample size of our study is limited; studies we have already initiated will include a larger number of piglets to establish statistical differences between treatment strategies.

Previous MSC treatments in swine models has demonstrated benefit for myocardial infarction[56] and defects in articular cartilage[57]; however, there are no published reports of autologous porcine UC MSCs to treat bone defects. Although based on a small sample size secondary to the high cost of swine subjects, our preliminary study is the first to demonstrate use of autologous UC MSCs for bone regeneration *in vivo*. In addition, our study is the first to reveal successful bone regeneration in a critical-sized maxillary defect with use of predifferentiated MSCs.

Conclusions

A novel, reproducible, critical-sized alveolar cleft swine model is presented with three treatment alternatives including a successful tissue-engineered treatment with UC MSCs on PLGA NMFS. The swine model appears to be a strong platform for *in vivo* testing of engineered bone, with the novel therapy favorably comparing to cancellous bone grafting, the current gold standard treatment. To prepare the foundation for clinical studies using UC MSCs, we are now expanding the number of test animals, and extending the time frame for follow-up. This strategy should give us more definitive evidence of the efficacy of this novel stem cell-based treatment.

Acknowledgment

This study was supported by grant from the National Institute of Dental and Craniofacial Research (NIDCR) and the Plastic Surgery Education Foundation.

Disclosure Statement

No competing financial interests exist.

References

1. Eppley, B.L., *et al.* The spectrum of orofacial clefting. Plast Reconstr Surg **115,** 101e, 2005.
2. Cohen, S.R., *et al.* American society of maxillofacial surgeons outcome study: preoperative and postoperative neurodevelopmental findings in single-suture craniosynostosis. Plast Reconstr Surg **114,** 841; discussion 848, 2004.
3. van Aalst, J.A., *et al.* Surgical technique for primary alveolar bone grafting. J Craniofac Surg **16,** 706, 2005.
4. Friede, H., and Johanson, B. A follow-up study of cleft children treated with primary bone grafting. 1. Orthodontic aspects. Scand J Plast Reconstr Surg **8,** 88, 1974.
5. Daskalogiannakis, J., *et al.* The Americleft study: an inter-center study of treatment outcomes for patients with unilateral cleft lip and palate part 3. Analysis of craniofacial form. Cleft Palate Craniofac J **48,** 252, 2011.
6. Long, R.E., Jr., *et al.* The Americleft study: an inter-center study of treatment outcomes for patients with unilateral cleft lip and palate part 1. Principles and study design. Cleft Palate Craniofac J **48,** 239, 2011.

7. Buchman, S.R., and Ozaki, W. The ultrastructure and resorptive pattern of cancellous onlay bone grafts in the craniofacial skeleton. Ann Plast Surg **43,** 49, 1999.
8. Meazzini, M.C., *et al.* A cephalometric intercenter comparison of patients with unilateral cleft lip and palate: analysis at 5 and 10 years of age and long term. Cleft Palate Craniofac J **45,** 654, 2008.
9. Banwart, J.C., Asher, M.A., and Hassanein, R.S. Iliac crest bone graft harvest donor site morbidity. A statistical evaluation. Spine (Phila Pa 1976) **20,** 1055, 1995.
10. Rosenthal, A.H., and Buchman, S.R. Volume maintenance of inlay bone grafts in the craniofacial skeleton. Plast Reconstr Surg **112,** 802, 2003.
11. Dubel, H., and Honigmann, K. [Psychology and recurrence tendency in relation to age at operation for prognathism]. Swiss Dent **13,** 15; 17, 1992 [Article in German].
12. Landsberger, P., *et al.* Evaluation of patient satisfaction after therapy of unilateral clefts of lip, alveolus and palate. J Craniomaxillofac Surg **34 Suppl 2,** 31, 2006.
13. Panetta, N.J., *et al.* Tissue engineering in cleft palate and other congenital malformations. Pediatr Res **63,** 545, 2008.
14. Raposo-Amaral, C.E., *et al.* Is bone transplantation the gold standard for repair of alveolar bone defects? J Tissue Eng **5,** 2041731413519352, 2014.
15. Kawata, T., *et al.* New biomaterials and methods for craniofacial bone defect: chondroid bone grafts in maxillary alveolar clefts. J Craniofac Genet Dev Biol **20,** 49, 2000.
16. de Ruiter, A., *et al.* beta-TCP versus autologous bone for repair of alveolar clefts in a goat model. Cleft Palate Craniofac J **48,** 654, 2011.
17. El-Deeb, M., Horswell, B., and Waite, D.E. A primate model for producing experimental alveolar cleft defects. J Oral Maxillofac Surg **43,** 523, 1985.
18. Henkel, K.O., *et al.* Closure of vertical alveolar bone defects with guided horizontal distraction osteogenesis: an experimental study in pigs and first clinical results. J Craniomaxillofac Surg **29,** 249, 2001.
19. Lawson, R.B., and Jones, M.L. An evaluation of a noninvasive method of assessing alveolar bone levels in an experimental model of cleft lip and palate. Cleft Palate Craniofac J **35,** 1, 1998.
20. Herring, S.W., *et al.* Temporomandibular joint in miniature pigs: anatomy, cell replication, and relation to loading. Anat Rec **266,** 152, 2002.
21. Mars, M., and Houston, W.J. A preliminary study of facial growth and morphology in unoperated male unilateral cleft lip and palate subjects over 13 years of age. Cleft Palate J **27,** 7, 1990.
22. Swindle, M.M.E. Swine in the Laboratory: Surgery, Anesthesia, Imaging, and Experimental Techniques. Second edition. Swindle, M.M., ed. Boca Raton, FL: CRC Press, 2007, p. 496.
23. Stembirek, J., *et al.* The pig as an experimental model for clinical craniofacial research. Lab Anim **46,** 269, 2012.
24. International Swine Genome Sequencing Consortium. Pig genome sequence strategy. Accessed 2014. www.piggenome.org.
25. Prather, R.S., *et al.* Genetically engineered pig models for human diseases. Annu Rev Anim Biosci **1,** 203, 2013.
26. Chung, V.H., *et al.* Engineered autologous bone marrow mesenchymal stem cells: alternative to cleft alveolar bone graft surgery. J Craniofac Surg **23,** 1558, 2012.
27. Donovan, M.G., *et al.* Autologous calvarial and iliac onlay bone grafts in miniature swine. J Oral Maxillofac Surg **51,** 898, 1993.
28. Yushkevich, P.A., *et al.* User-guided 3D active contour segmentation of anatomical structures: significantly improved efficiency and reliability. Neuroimage **31,** 1116, 2006.
29. Dahl, J.P., *et al.* Analysis of human auricular cartilage to guide tissue-engineered nanofiber-based chondrogenesis: implications for microtia reconstruction. Otolaryngol Head Neck Surg **145,** 915, 2011.
30. Caballero, M., *et al.* Osteoinduction in umbilical cord- and palate periosteum-derived mesenchymal stem cells. Ann Plast Surg **64,** 605, 2010.
31. Reed, C.R., *et al.* Composite tissue engineering on polycaprolactone nanofiber scaffolds. Ann Plast Surg **62,** 505, 2009.
32. Caballero, M., *et al.* Osteoinduction of umbilical cord and palate periosteum-derived mesenchymal stem cells on poly(lactic-co-glycolic) acid nanomicrofibers. Ann Plast Surg **72,** S176, 2014.
33. Saka, B., *et al.* Blood supply of the mandibular cortex: an experimental study in Gottingen minipigs with special reference to the condyle. J Craniomaxillofac Surg **30,** 41, 2002.
34. Carls, F.R., *et al.* Prefabrication of mucosa-lined flaps: a preliminary study in the pig model. Plast Reconstr Surg **101,** 1022, 1998.
35. Docherty-Skogh, A.C., *et al.* Bone morphogenetic protein-2 delivered by hyaluronan-based hydrogel induces massive bone formation and healing of cranial defects in minipigs. Plast Reconstr Surg **125,** 1383, 2010.
36. Lin, Y.Y., *et al.* The mandibular cartilage metabolism is altered by damaged subchondral bone from traumatic impact loading. Ann Biomed Eng **37,** 1358, 2009.
37. Grehan, J.F., *et al.* Development and evaluation of a swine model to assess the preclinical safety of mechanical heart valves. J Heart Valve Dis **9,** 710; discussion 719, 2000.
38. Wheeler, D.G., *et al.* Transgenic swine: expression of human CD39 protects against myocardial injury. J Mol Cell Cardiol **52,** 958, 2012.
39. Lai, L., *et al.* Transgenic pig expressing the enhanced green fluorescent protein produced by nuclear transfer using colchicine-treated fibroblasts as donor cells. Mol Reprod Dev **62,** 300, 2002.
40. Huang, J., *et al.* RAG1/2 knockout pigs with severe combined immunodeficiency. J Immunol **193,** 1496, 2014.
41. Zheng, Y., *et al.* Stem cells from deciduous tooth repair mandibular defect in swine. J Dent Res **88,** 249, 2009.
42. Hughes, G.C., Post, M.J., Simons, M., and Annex, B.H. Translational physiology: porcine models of human coronary artery disease: implications for preclinical trials of therapeutic angiogenesis. J Appl Physiol **94,** 1689, 2003.
43. Üstüner, E.T., *et al.* Swine composite tissue allotransplant model for preclinical hand transplant studies. Microsurgery **20,** 400, 2000.
44. Thorwarth, M., *et al.* Expression of bone matrix proteins during de novo bone formation using a bovine collagen and platelet-rich plasma (prp)—an immunohistochemical analysis. Biomaterials **26,** 2575, 2005.
45. Papadaki, M.E., *et al.* A minipig model of maxillary distraction osteogenesis. J Oral Maxillofac Surg **68,** 2783, 2010.
46. Schmitz, J.P., and Hollinger, J.O. The critical size defect as an experimental model for craniomandibulofacial nonunions. Clin Orthop Relat Res 299, 1986.
47. Szpalski, C., *et al.* Cranial bone defects: current and future strategies. Neurosurg Focus **29,** E8, 2010.

48. Collins, M., James, D.R., and Mars, M. Alveolar bone grafting: a review of 115 patients. Eur J Orthod **20,** 115, 1998.
49. Shirota, T., *et al.* Analysis of bone volume using computer simulation system for secondary bone graft in alveolar cleft. Int J Oral Maxillofac Surg **39,** 904, 2010.
50. Fong, C.Y., *et al.* Derivation efficiency, cell proliferation, freeze-thaw survival, stem-cell properties and differentiation of human Wharton's jelly stem cells. Reprod Biomed Online **21,** 391, 2010.
51. Mesenchymal stem cells clinical trials. NIH. https://clinicaltrials.gov. 2013.
52. Noort, W.A., *et al.* Human versus porcine mesenchymal stromal cells: phenotype, differentiation potential, immunomodulation and cardiac improvement after transplantation. J Cell Mol Med **16,** 1827, 2012.
53. van Aalst, J.A., *et al.* Cellular incorporation into electrospun nanofibers: retained viability, proliferation, and function in fibroblasts. Ann Plast Surg **60,** 577, 2008.
54. Gilardino, M.S., Chen, E., and Bartlett, S.P. Choice of internal rigid fixation materials in the treatment of facial fractures. Craniomaxillofac Trauma Reconstr **2,** 49, 2009.
55. Vaccaro, A.R. The role of the osteoconductive scaffold in synthetic bone graft. Orthopedics **25 (5 Suppl),** s571, 2002.
56. Shake, J.G. *et al.* Mesenchymal stem cell implantation in a swine myocardial infarct model: engraftment and functional effects. Ann Thorac Surg **73,** 1919; discussion 1926, 2002.
57. Li, W.J., *et al.* Evaluation of articular cartilage repair using biodegradable nanofibrous scaffolds in a swine model: a pilot study. J Tissue Eng Regen Med **3,** 1, 2009.

Address correspondence to:
John A. van Aalst, MD
Division of Craniofacial and Pediatric Plastic Surgery
Cincinnati Children's Hospital Medical Center
3333 Burnet Avenue
Cincinnati, OH 45229

E-mail: john.vanaalst@cchmc.org

Received: November 21, 2014
Accepted: March 5, 2015
Online Publication Date: July 14, 2015